2021

A Step Closer to Elastogenesis on Demand; Inducing Mature Elastic Fibre Deposition in a Natural Biomaterial Scaffold

Francisco R. Almeida-González
Technological University Dublin

Arlyng González-Vázquez
RCSI University of Medicine, Ireland

Suzanne M. Mithieux
Charles Perkins Centre, University of Sydney, Australia

See next page for additional authors

Recommended Citation

Almeida-Gonz´alez et al. (2021) A Step Closer to Elastogenesis on Demand; Inducing Mature Elastic Fibre Deposition in a Natural Biomaterial Scaffold, *Materials Science and Engineering: C,* Volume 120, January, doi:10.1016/j.msec.2020.111788

Materials Science & Engineering C 120 (2021) 111788

Contents lists available at ScienceDirect

Materials Science & Engineering C

journal homepage: www.elsevier.com/locate/msec

A step closer to elastogenesis on demand; Inducing mature elastic fibre deposition in a natural biomaterial scaffold

Francisco R. Almeida-González [a,b], Arlyng González-Vázquez [b,c], Suzanne M. Mithieux [d,e,f], Fergal J. O'Brien [b,c], Anthony S. Weiss [d,e,f], Claire M. Brougham [a,b,*]

[a] Biomedical Research Group, School of Mechanical and Design Engineering, Technological University Dublin, Bolton St, Dublin 1, Ireland
[b] Tissue Engineering Research Group, Dept. of Anatomy and Regenerative Medicine, RCSI University of Medicine and Health Sciences, 123 St. Stephen's Green, Dublin 2, Ireland
[c] Advanced Materials and Bioengineering Research (AMBER) Centre, RCSI, Ireland
[d] Charles Perkins Centre, University of Sydney, NSW 2006, Australia
[e] School of Life and Environmental Sciences, University of Sydney, NSW 2006, Australia
[f] Bosch Institute, University of Sydney, NSW 2006, Australia

ARTICLE INFO

Keywords:
Collagen scaffold
Smooth muscle cells
Elastogenesis
Elastic fibre
Tropoelastin

ABSTRACT

Elastic fibres play a key role in bodily functions where fatigue resistance and elastic recovery are necessary while regulating phenotype, proliferation and migration in cells. While *in vivo* elastic fibres are created at a late foetal stage, a major obstacle in the development of engineered tissue is that human vascular smooth muscle cells (hVSMCs), one of the principal elastogenic cells, are unable to spontaneously promote elastogenesis *in vitro*. Therefore, the overall aim of this study was to activate elastogenesis *in vitro* by hVSMCs seeded in fibrin, collagen, glycosaminoglycan (FCG) scaffolds, following the addition of recombinant human tropoelastin. This combination of scaffold, tropoelastin and cells induced the deposition of elastin and formation of lamellar maturing elastic fibres, similar to those found in skin, blood vessels and heart valves. Furthermore, higher numbers of maturing branched elastic fibres were synthesised when a higher cell density was used and by drop-loading tropoelastin onto cell-seeded FCG scaffolds prior to adding growth medium. The addition of tropoelastin showed no effect on cell proliferation or mechanical properties of the scaffold which remained dimensionally stable throughout. With these results, we have established a natural biomaterial scaffold that can undergo controlled elastogenesis on demand, suitable for tissue engineering applications.

1. Introduction

Fatigue resistance and elastic recovery are critically important mechanical properties for the correct functioning of the heart, skin, lungs and other dynamic connective tissues within the human body. Elastic fibres play a key role in bodily functions where these mechanical properties are necessary [1]. Indeed, elastin is one of the most abundant proteins found in vertebrates, providing resistance to permanent tissue deformation [2] and delivering biochemical cues that regulate cell migration, preventing proliferative diseases in heart and blood vessels [3,4]. In a mature elastic fibre, approximately 90% of the volume is composed of elastin that is surrounded by a fibrillin-rich microfibrillar mesh [5]. However, the content, alignment and morphology of these mature elastic fibres is dictated by functional demands and the cells that deposit and orientate the fibrillin-rich microfibrils. For instance, elastic ligaments have approximately 50% elastin content [6] with elastic fibres that resemble rope-like networks giving joints stability and flexibility. Blood vessels have a 30% elastin content, and the elastic fibres can be observed as concentric fenestrated lamellae required for stress propagation during each cardiac cycle. Having 15% of elastin content, heart valves show a mixed architecture of elastic fibres; while the ventricularis layer of the leaflets has elastic fibres aligned radially to withstand the blood inflow [7], reticular elastic fibres are present throughout the heart valve to reduce permanent deformation [8]. Lungs on the other hand (3–7% elastin), present elastic fibres that are highly branched along the respiratory tree and facilitate alveoli expansion. Finally, skin, which contains approximately 2% of elastin [9], has elastic fibres that are thick and horizontally arranged in the dermis, whereas in the papillary

* Corresponding author at: Technological University Dublin, Bolton Street, D01 K822, Ireland.
E-mail address: claire.brougham@TUDublin.ie (C.M. Brougham).

https://doi.org/10.1016/j.msec.2020.111788
Received 29 July 2020; Received in revised form 20 November 2020; Accepted 2 December 2020
Available online 10 December 2020

dermis, these fibres are perpendicularly oriented [10]. While many biocompatible materials have been developed for tissue engineering applications, to date they are unable to fully mimic the function of native tissue, as they do not encourage the production of new elastic fibres through elastogenesis [11].

Elastogenesis is a hierarchical elastic fibre assembly process that is highly upregulated at late foetal and neonatal stage [12]. Tropoelastin, the soluble precursor of elastin, is essential for the assembly of elastic fibres [6]. In a normal elastogenesis process, cells produce tropoelastin that is chaperoned by elastin-binding proteins (EBP) to prevent premature coacervation into elastin [13]. When tropoelastin leaves the cellular membrane, it coacervates into elastin chains within the extracellular matrix (ECM). Elastin then begins to crosslink using lysyl oxidase (LOX1), copper, fibulin 4 and 5 to make insoluble elastin that is finally deposited in the microfibrillar mesh [12], allowing elastic fibres to form with a lifespan of approximately 70 years [14,15]. From the estimated 200 cell types found in the human body [16], only smooth muscle cells, fibroblasts, endothelial cells, chondroblasts and mesothelial cells are capable of assembling elastic fibres *in vivo* [17]. However, a major issue for researchers is that these cells are unable to spontaneously undergo elastogenesis *in vitro*.

Indeed, much research in recent years has focused on finding ways to induce elastogenesis in cell culture using exogenous agents [18]. *In vitro*, glycosaminoglycans (GAGs) such as heparin [19], hormones, growth factors [20–23] and gene expression therapy [24] can induce production of tropoelastin in cells and upregulation of microfibrillar associated genes, leading to the formation of elastic fibres in fibroblasts and smooth muscle cells (SMCs). Another way of obtaining elastic fibres *in vitro* is by adding a solution of recombinant human tropoelastin that can be incorporated into the ECM, thereby skipping the tropoelastin synthesis phase inside the cell [12,17,25,26]. Additionally, it has been well-documented that similarly to natural tropoelastin, recombinant human tropoelastin can modulate the assembly of elastic fibres in the ECM, while promoting attachment of cells and regulating their proliferation [1,27–30]. Recently, Mithieux et al. presented ways of obtaining elastic fibres in silicone and collagen constructs. This was achieved through repeated additions of recombinant synthetic human tropoelastin and conditioned growth medium, using dermal fibroblasts of different age groups [31]. As a result of these findings, there is a need to examine whether this technique can be translated into other cell-seeded biomaterial constructs. Additionally, the effect of the method and timing of recombinant human tropoelastin addition, on the deposition of elastic fibres, warrants examination.

Our research group is specialised in the fabrication of natural polymer based porous scaffolds, for several medical applications including cartilage [32,33], bone [34], nerve [35], and vascular [36] repair. We have developed a platform for soft tissue engineering that can resist cell-mediated contraction using fibrin gels reinforced with a freeze-dried collagen-glycosaminoglycan matrix [37]. Although these fibrin-collagen-glycosaminoglycan (FCG) scaffolds have proven to be dimensionally stable in cell culture when seeded with smooth muscle cells, the next step is to develop a repeatable method to increase and tune the content of elastic fibres when cultured with appropriate cells. This milestone will take us a step closer to meeting the unmet need of a fully functional natural biomaterial scaffold, able to undergo elastogenesis on demand, with increased elastic recoil and fatigue life. Such a biomaterial may prove suitable for a variety of applications.

Therefore, the overall aim of this study was to activate elastogenesis by human vascular smooth muscle cells (hVSMCs) seeded in the FCG scaffolds. We established the influence of the timing of tropoelastin addition on the maturing elastic fibre deposition, cell proliferation and gene expression of hVSMCs seeded on glass slides. Next, we assessed the effect of changing the method of addition of tropoelastin on the deposition and area coverage of elastin and maturing elastic fibres in FCG scaffolds seeded with hVSMCs. Finally, we studied the effect of controlled elastogenesis on the cell proliferation, mechanical and dimensional properties and elastogenesis associated gene expression in FCG scaffolds seeded with hVSMCs.

2. Materials and methods

2.1. Cell culture

A human vascular smooth muscle cell line (hVSMC) from an 11-month female Caucasian (CRL-1999, ATCC, Middlesex, UK), was cultured in growth medium composed of F-12K Medium (ATCC), with added 50 μg/ml ascorbic acid, 16 μl/ml Insulin, Transferrin, Selenium (ITS, Sigma-Aldrich), 30 μg/ml Endothelial Cell Growth Supplement (ECGS, Sigma-Aldrich), 10% foetal bovine serum, 1% penicillin/streptomycin, 10 mM, 4-(2-hydroxyethyl)-1-piperazineethanesulfonic acid (HEPES, Sigma-Aldrich) and 10 mM 2-[(2-Hydroxy-1,1-bis(hydroxymethyl)ethyl)amino]ethanesulfonic acid, N-[Tris(hydroxymethyl) methyl]-2-aminoethanesulfonic acid (TES, Sigma-Aldrich). Growth medium was replaced every three days and cells sub-cultured, once fully confluent, using 0.25% trypsin 0.53 mM EDTA solution (Sigma-Aldrich).

2.2. Tropoelastin solution preparation

For these experiments, recombinant synthetic human tropoelastin without hydrophilic domain 26A (SHELΔ26A) (amino acid residues 27–724 of GenBank entry AAC98394). The production process involved overexpression of tropoelastin in *Escherichia coli* followed by purification and this has been previously described [38,39]. The resultant lyophilised tropoelastin was dissolved overnight in phosphate buffer saline (PBS, Sigma-Aldrich), to obtain a 10 mg/ml solution.

2.3. 2D elastogenesis model

To assess the optimal timing of tropoelastin addition in order to enhance the deposition of more elastic fibres, two groups were studied. Samples were treated with tropoelastin on day 0 (A0) and further samples were treated on day 10 (A10), as the rationale in this model is that a mature ECM would enhance the deposition of elastin and maturing elastic fibres. Therefore, hVSMCs were seeded in 12-well plates containing glass cover slips at a density of approximately 50,000 cells per well. 50 μl of 10 mg/ml tropoelastin was added to all the samples on their designated day. After adding growth medium, the final concentration of tropoelastin per well was 250 μg/ml. Growth medium changes were carried out on days 3 and 5 of the experiment. Samples were collected on days 1, 3 and 7 post-tropoelastin addition for cell number quantification, real-time quantitative PCR (RT-qPCR), immunofluorescence (anti-elastin) and maturing elastic fibre autofluorescence at 561 nm [31].

2.4. Elastin and elastic fibre area coverage estimation

Immunofluorescence was carried out to visually assess for the presence of elastin and maturing elastic fibres. Samples were fixated with 10% formalin for 15 min, washed twice in PBS and three times with 0.2 M Glycine (Sigma-Aldrich). Samples were incubated for 1 h at 37 °C in 5% *w/v* bovine serum albumin (Sigma-Aldrich), kept in the fridge overnight with 1:100 BA4 anti-elastin antibody (Abcam, Cambridge, UK), incubated with 1:500 Alexa Fluor® 488 (Abcam) for 1 h at 37 °C. Glass microscope slides and Fluoroshield with DAPI (Sigma-Aldrich) were used to mount the 2D samples while 3D samples were kept in glycine. Elastin was observed at 488 nm (green channel) and maturing elastic fibres (covalently cross-linked elastin) were visualised at a wavelength of 561 nm (red channel) using a confocal microscope, due to its autofluorescence. The following calculations were carried out using the image processing package, Fiji [40]. Relative area coverage was carried out by thresholding the elastin and maturing elastic fibres channels and quantifying the intensity of each pixel ($n = 4$). Maturing

elastic fibre alignment was assessed by smoothing the respective channel and analysing it using the directionality function, which estimates the preferred orientation of clusters of pixels in the image using the Fourier spectrum analysis method.

2.5. Cell number quantification

To investigate the influence of tropoelastin on the proliferation of hVSMCs, a Quant-iT PicoGreen dsDNA kit (BD BioSciences, Oxford, UK) was used. This kit can detect double-stranded DNA (dsDNA) through fluorescence imaging. Samples ($n = 3$ for each time point) were washed in PBS and kept at −20 °C in a solution of 0.2 M $NaCO_3$ and 1% Triton X (Sigma-Aldrich). Each sample was diluted 25× with 1xTE Buffer, pipetted into a 96-well plate and treated with a 200-fold PicoGreen dilution. Using a TECAN plate reader, samples were excited at 485 nm and read at 538 nm. dsDNA concentration was calculated by comparing the fluorescence levels from each sample against a standard fluorescence curve [41].

2.6. Elastogenesis associated gene expression

To evaluate the influence of tropoelastin on the gene expression of elastin (ELN), elastin-binding protein (EBP), fibrillin 1 (FBN1) and lysyl oxidase (LOX1) genes (ELN QT00034594, EBP1 QT00087570, FBN1 QT00024507, LOX1 QT00017311, Qiagen, Manchester, UK) RT-qPCR was carried out. Three samples per group ($n = 3$) at each of the time points were washed in PBS and kept at −20 °C with Qiazol lysis reagent (Qiagen). RNA was extracted and reverse transcription carried out with a Quantitec Reverse Transcription kit (Qiagen). The resultant complementary DNA (cDNA) samples were prepared with PCR Master Mix (Bioline, London, UK) and analysed using an Eppendorf® Mastercycler® ep realplex 4 with the following program: 15 min at 95 °C, 15 s at 94 °C, 30 s at 55 °C, 45 s at 72 °C (the previous three steps repeated 40 cycles), 15 s at 95 °C, 15 s at 60 °C, 20 min melting curve and 15 s at 95 °C. Glyceraldehyde 3-phosphate dehydrogenase (GAPDH, QT00079247, Qiagen) was used as the housekeeping gene and relative fold gene expression of samples was calculated using the $2^{-\Delta\Delta Ct}$ method [42].

2.7. 3D elastogenesis model

2.7.1. Fabrication of cell-seeded FCG scaffolds

To create FCG scaffolds, a collagen-GAG (CG) matrix was created and infiltrated with fibrin. Briefly, CG scaffolds (⌀ 10 mm × 5 mm discs) were fabricated by freeze-drying a solution of 0.05 M glacial acetic acid containing 0.75% w/v type I bovine tendon collagen (Southern Lights Biomaterials, New Zealand) and 0.044% w/v shark cartilage chondroitin-6-sulfate (Sigma-Aldrich). Final freezing temperature was set at −10 °C to create scaffolds with an average pore size of 120 μm [43]. CG scaffolds were physically cross-linked using dehydrothermal treatment (DHT) [44], then chemically cross-linked using 1-ethyl-3–3-dimethyl aminopropyl carbodiimide (EDAC), N-hydroxysuccinimide (NHS) (Sigma–Aldrich) and ethanol [45]. Fibrin gel components were fabricated as previously described [37]. To fabricate acellular FCG scaffolds, tris-buffered saline (pH 7.4), 50 mM $CaCl_2$, 40 IU/ml thrombin (Sigma-Aldrich) and 10 mg/ml of fibrinogen, were pipetted into the scaffolds. To fabricate cell-seeded FCG scaffolds, hVSMCs (density of 1000 cells/mm^3) were mixed with 10 mg/ml of fibrinogen and added into each scaffold. To reduce the speed of the enzymatic degradation of fibrin, the growth medium contained 20 μg/ml of aprotinin (Sigma-Aldrich) [46]. We will refer to cell-seeded FCG scaffolds as FCG scaffolds from here on.

2.7.2. Method of tropoelastin addition to FCG scaffolds

Once the cells had been proliferating in the scaffolds for 7 days, we assessed the effect that the method of tropoelastin addition had on the formation of elastin and elastic fibres. We removed the growth medium from the wells and used two methods to add tropoelastin to the FCG scaffolds: 1) drop-loading 50 μl of 10 mg/ml tropoelastin onto the scaffolds, waiting 10 min before adding fresh growth medium and 2) adding growth medium which already contained 50 μl of 10 mg/ml of tropoelastin. In both cases, the final concentration of tropoelastin per well was 250 μg/ml. It is worth mentioning that concentration dependency studies were not carried out using our scaffolds, therefore the concentration of tropoelastin chosen for this study was based on a previous recombinant human tropoelastin publication [31]. Growth medium changes were carried out every 3 days. Seven days post initial tropoelastin addition, a second round of tropoelastin was added onto the FCG scaffolds using the two methods described above. Samples were collected on days, 3, 7 and 14 (post initial tropoelastin addition) for dsDNA quantification, RT-qPCR, immunofluorescence (anti-elastin) and autofluorescence at 561 nm, as described in previous paragraphs ($n = 3$ for all assays).

2.7.3. Quantification of elastin deposited within the FCG scaffolds

The Fastin™ Elastin Assay kit (Biocolor Ltd., Carrickfergus, UK) was used to quantify the amount of elastin deposited in FCG scaffolds. Briefly, FCG scaffolds ($n = 4$) were collected on days 3, 7 and 14, washed 3 times in PBS and weighed. For the extraction of soluble α-elastin, FCG scaffolds were fully digested in 0.25 M oxalic acid for 1 h at 100 °C. Following elastin solubilisation, 500 μl from each sample was precipitated, centrifuged and mixed with dye reagent. The resultant elastin-dye complex was centrifuged and the pellet solubilised using the dye dissociation agent. Samples were transferred to a clear 96-well plate and absorbance at 513 nm was measured using the plate reader. Observations were normalised to the corresponding blanks (0.25 M oxalic acid) and expressed in μg of elastin per 100 mg of wet scaffold.

2.7.4. Mechanical characterisation of FCG scaffolds

FCG scaffolds ($n = 3$) soaked in PBS were compressed uniaxially, perpendicular to their flat face, to 10% strain at 0.1% strain per second. The compressive modulus was obtained by calculating the slope of the stress-strain curves [47]. Dog bone-shaped FCG scaffolds (n = 3, only day 14 samples due to cell numbers involved), as per ASTM D638, were hydrated in PBS and tested using a tensile preload of 0.01 N at a tension rate of 5 mm/min until failure. Tests were carried out using a universal testing machine (Zwick/Roell) fitted with a 5 N load cell. Ultimate tensile strength, strain to failure, low strain (2–5%) and high strain (10–15%) tensile modulus were calculated from the stress-strain curves generated [48]. To assess the effect of the addition of tropoelastin on the dimensional integrity of FCG scaffolds, they ($n = 3$) were photographed using a digital camera, and their diameter was measured using the image processing package, Fiji [40].

2.8. Statistical analyses

Results are expressed as mean ± standard deviation. Two-way analysis of variance (ANOVA) and Bonferroni post-test were carried out to analyse dsDNA concentration, gene relative fold change, elastin quantification, elastin coverage area, maturing elastic fibre coverage area, compressive modulus and dimensional integrity. t-test and Mann-Whitney *U* test was carried out to assess tensile modulus results. All results were compared against untreated samples (no tropoelastin added) and $P < 0.05$ was defined as statistically significant.

3. Results

3.1. Mature ECM enhanced elastogenesis

Samples on glass slides were treated with tropoelastin on day 0 (A0) and further samples were treated on day 10 (A10) based on the hypothesis that a higher density of cells may result in more ECM synthesis and this would enhance the deposition of elastin and maturing elastic

fibres. Indeed, elastin and maturing elastic fibre deposition was visible on day 3 in A10 samples (Fig. 1E), with a steady and significant deposition of elastin (Fig. 1F, G) and maturing elastic fibres (Fig. 1J, K) on days 7 and 14. A0 samples on the other hand, showed a small amount of elastin on day 3, however no elastin or maturing elastic fibres were observed at any other time point. As expected, samples with no tropoelastin added, showed no elastin or maturing elastic fibres during the experiment (Fig. 1A-D, H).

To quantify the elastin and maturing elastic fibres observed, measurements of the relative area coverage of both were carried out using image analysis software. As expected, A10 samples had a significantly higher content of elastin and maturing elastic fibres than A0 samples (Fig. 2). On day 3, 13% of the surface area of the A10 samples was covered by elastin ($p < 0.001$) and by day 14, this coverage increased to almost 20% ($p < 0.001$). When the coverage of maturing elastic fibres was measured on day 3, there was less than 1% coverage and by day 14 the coverage was approximately 8% ($p < 0.001$). In addition, assessment of fibre alignment in A10 samples showed a preferred orientation of the maturing elastic fibres as indicated by the directionality curves (Fig. 2C). We have proven that a mature ECM increased significantly the deposition of elastin and maturing elastic fibres in hVSMCs seeded on glass slides.

3.1.1. Tropoelastin regulated cell proliferation

The effect of tropoelastin on the proliferation of hVSMCs was measured using a PicoGreen assay over a 1-week period. Untreated samples presented a higher cell proliferation rate ($p < 0.001$) when compared to A0 and A10 samples (Fig. 3). On day 1, A0 samples and A10 samples had a mean dsDNA concentration of 242 ± 53 ng/ml and 297 ± 36 ng/ml respectively, while the untreated samples were measured at 219 ± 46 ng/ml. Within three days of treatment, dsDNA concentration remained constant; 247 ± 0.3 ng/ml in A0 samples, 315 ± 117 ng/ml in A10 samples and 228 ± 09 ng/ml in untreated samples. Untreated samples showed a significantly higher dsDNA concentration (658 ± 117 ng/ml) than A0 samples (469 ± 27 ng/ml) and A10 samples (332 ± 13 ng/ml) after seven days. These results demonstrate that tropoelastin regulates the proliferation of hVSMCs seeded on glass slides regardless of cell density levels.

3.1.2. Tropoelastin addition triggered elastogenesis

Having assessed cell proliferation on glass slides, the next step was to study the effect of the day of addition of tropoelastin on the expression of the elastin (ELN), lysyl oxidase-1 (LOX1), elastin binding protein (EBP) and fibrillin-1 (FBN1) genes in hVSMCs. One day after the addition of tropoelastin in A0 samples, there was a slight upregulation of LOX1 (1.2 ± 0.03) and EBP (1.3 ± 0.5), whereas ELN and FBN1 remained unchanged. Samples collected on day 3 presented upregulation of ELN (1.3 ± 0.7), LOX1 (1.5 ± 0.5) EBP (1.3 ± 0.2) and FBN1 (1.4 ± 0.4) (Fig. 4A, B, D). Downregulation of ELN, LOX1 and FBN1 occurred on day 7, however EBP (1.3 ± 0.1) remained upregulated.

On the other hand, in A10 samples on day 1, there was downregulation of ELN (0.3 ± 0.3), LOX1 (0.5 ± 0.1), EBP (0.8 ± 0.6) and FBN1 (0.6 ± 0.3). Three days later upregulation of FBN1 (1.3 ± 2) occurred. We could see that on days 3 and 7, ELN and LOX remained downregulated. Furthermore, a relative fold change of 1.7 ± 1 in FBN1 and a 3-fold increase in EBP ($p < 0.001$) was observed after seven days (Fig. 4C). As there is no significant production of elastin or associated proteins (except EBP in A10 samples) by cells, we have demonstrated that elastogenesis was induced solely by adding tropoelastin on hVSMCs.

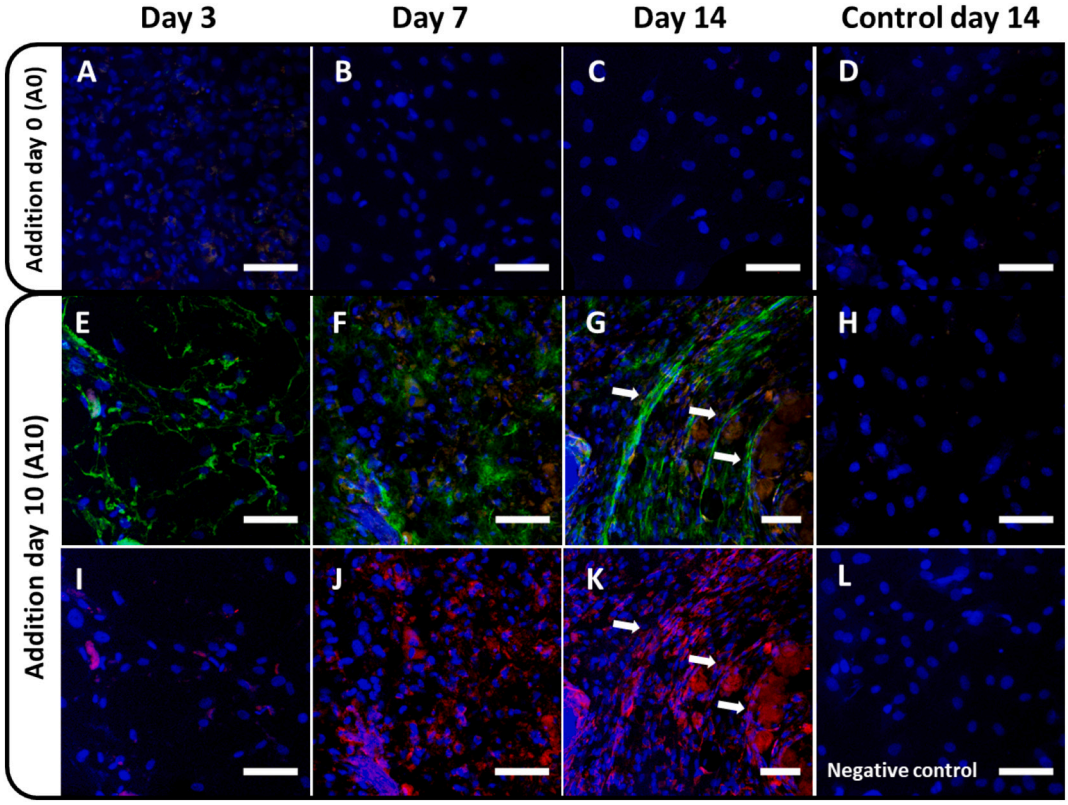

Fig. 1. Immunofluorescence of elastin (green) and autofluorescence at 561 nm of maturing elastic fibres (red) in hVSMCs treated with tropoelastin on A0 and A10 samples. A0 samples (A, B, C) did not show elastin or maturing elastic fibres. In contrast, both elastin (E, F, G) and maturing elastic fibres (I, J, K) were observed in A10 samples on days 3, 7 and 14. (D, H) Untreated samples imaged on day 14. (L) Sample treated with tropoelastin without primary antibody (negative control). White arrows represent lamellar-like elastic fibres. Blue = cell nuclei stained with DAPI. Scale bar represents 100 μm in all images. (For interpretation of the references to colour in this figure legend, the reader is referred to the web version of this article.)

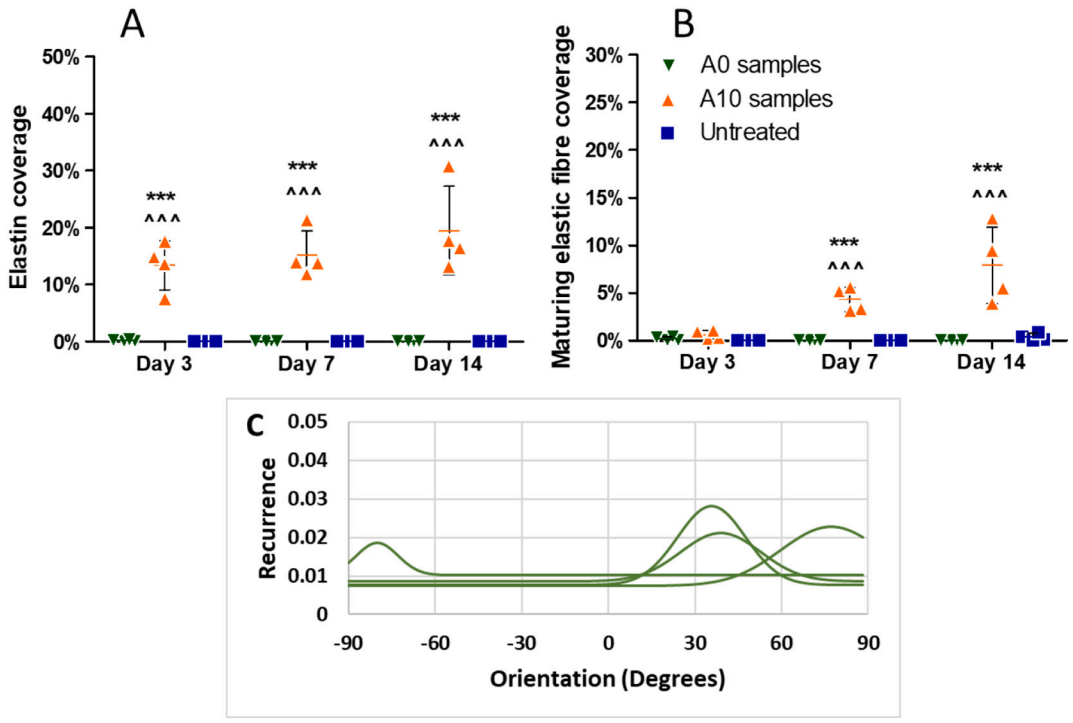

Fig. 2. Relative area coverage of elastin and maturing elastic fibres in A0 and A10 samples. There was a steady increase in (A) elastin and (B) maturing elastic fibre coverage in A10 samples at all time points. There was no evidence of elastin or maturing elastic fibres in A0 samples. (C) Directionality curves of maturing elastic fibres in A10 samples. Curves show a preferred orientation of maturing elastic fibres. (***) $p < 0.001$ when compared to A0 samples at the same time point. (^^^) $p < 0.001$ when compared to untreated samples.

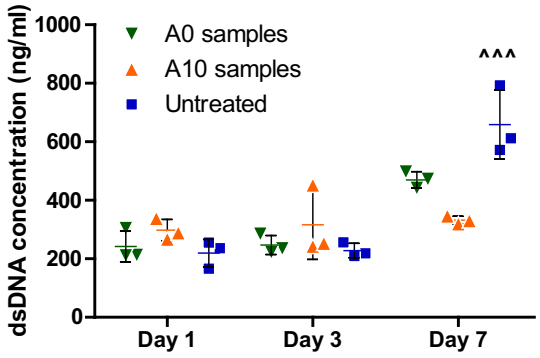

Fig. 3. Cell proliferation of hVSMCs seeded on glass slides treated with tropoelastin. dsDNA concentration slowly increased in A0, A10 and untreated samples. There was no difference between untreated and treated samples on days 1 and 3. On day 7 dsDNA concentration was significantly higher in untreated samples than A0 and A10 samples. (^^^) $p < 0.001$ when compared to A0 and A10 samples at the same time point.

3.2. Enhanced elastin deposition in FCG scaffold groups treated with tropoelastin

Having shown that higher density of cells resulted in a higher deposition of maturing elastic fibres (Fig. 2), we used this result when designing our 3D studies where we examined the effect of the method of addition of tropoelastin. The deposition of tropoelastin in FCG scaffolds was quantified using the Fastin™ Elastin Assay kit. On day 3, drop-loaded samples presented 223.5 ± 31 μg and media-loaded 224.2 ± 16 μg of elastin deposited per 100 mg of wet scaffold. Seven days after the initial addition of tropoelastin, there was approximately 194.4 ± 36 μg and 202 ± 31 μg in drop-loaded and media-loaded samples respectively. After the second addition of tropoelastin, there was no tangible increase in the overall content of elastin deposited in FCG scaffolds, therefore at the end of the experiment, the amount of tropoelastin was approximately 172.3 ± 37 μg in drop-loaded samples and 167.1 ± 28 μg in the media-loaded samples. Although there was a modest 10% reduction in elastin concentration per week, this drop in elastin was not significant. In contrast, significantly higher amounts of elastin were deposited in the groups treated with tropoelastin ($p < 0.001$) when compared against untreated samples (Fig. 5). These results demonstrate that tropoelastin can be deposited into cell-seeded FCG scaffolds and maintained without substantial losses.

3.2.1. Drop-loading tropoelastin improved the surface area coverage of maturing elastic fibres in FCG scaffolds

After quantifying the deposition of tropoelastin in FCG scaffolds as a function of the method of addition, we followed with the visual assessment of the surface area coverage of elastin and maturing elastic fibres in these scaffolds. Although the amount of elastin and maturing elastic fibres looked similar in drop-loaded and media-loaded samples (Fig. 6), there was a 4-fold increase in elastin ($p < 0.001$) and a 2-fold increase in maturing elastic fibre surface coverage ($p < 0.001$) in drop-loaded samples by day 14 ($p < 0.001$). Three days after the addition of tropoelastin, elastin was strikingly visible in both drop-loaded (Fig. 6A) and media-loaded (Fig. 6E) samples, appearing in both as elastin globules. However, by day 7 an unexpected decrease in this elastin content was observed (Fig. 6B, F). Interestingly, by day 14, maturing elastic fibres were visible in drop-loaded and media-loaded samples (Fig. 6B, F). At each time point cells were evenly distributed and not clumped. Acellular samples (Fig. 6H) and samples free from tropoelastin (Fig. 6D), did not present elastin or maturing elastic fibres.

Relative area coverage of elastin and maturing elastic fibres was quantified on the surface of the scaffolds, being significantly higher in the drop-loaded samples by the end of the experiment. Elastin coverage significantly increased in both drop-loaded (30 ± 9%) and media-loaded (24 ± 7%) samples on day 3 ($p < 0.001$), as can be seen in Fig. 7A. Day 7,

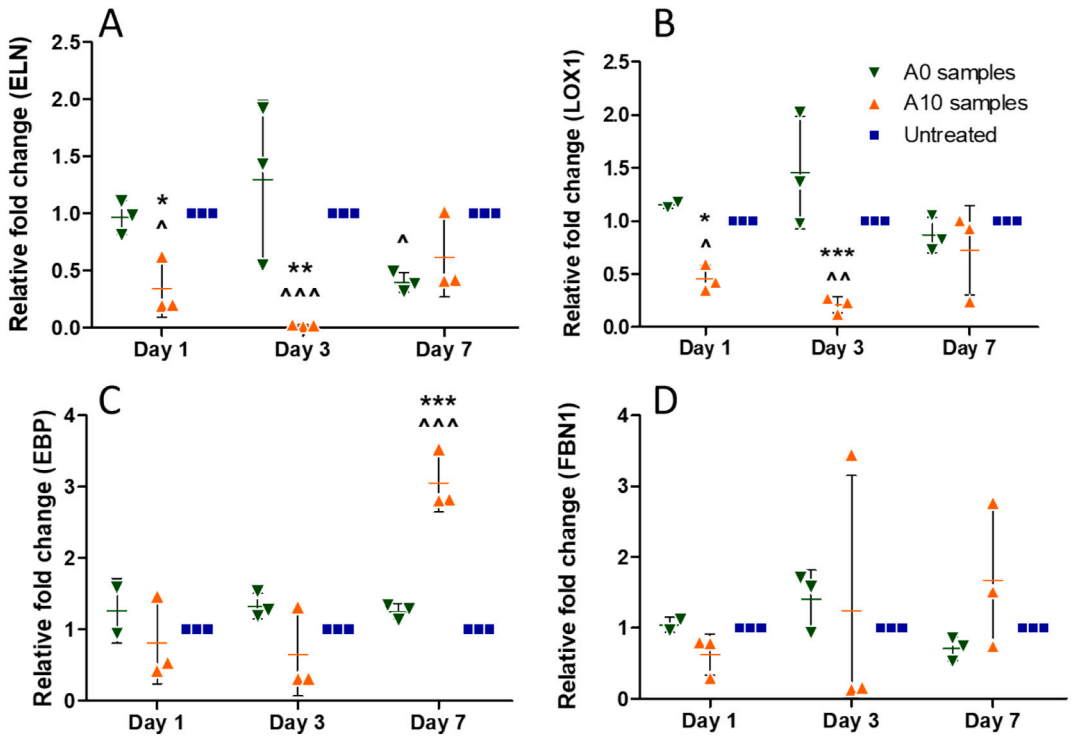

Fig. 4. Relative gene expression of ELN, LOX1, EBP and FBN1 in A0 and A10 samples. There was significant downregulation of (A) ELN and (B) LOX1 in A10 samples on days 1, 3 and 7. A 3-fold increase in (C) EBP expression in A10 samples was observed on day 7. There were no significant changes in (D) FBN1 expression. (^) $p < 0.05$, (^^) $p < 0.01$, (^^^) $p < 0.001$ when compared to untreated samples. (*) $p < 0.05$, (**) $p < 0.01$, (***) $p < 0.001$ when compared to A0 samples at the same time point.

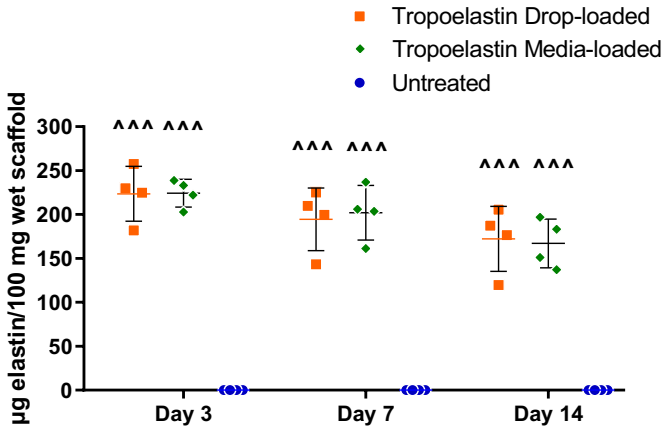

Fig. 5. Quantification of elastin deposited in FCG scaffolds. Drop-loaded and media-loaded samples presented significantly higher amounts of elastin deposited than untreated samples. (^^^) $p < 0.001$ when compared to untreated samples.

on the other hand, showed a drop, to approximately 2% in the elastin coverage area regardless of the method of addition. A second addition of tropoelastin increased the elastin coverage by day 14 up to 3 ± 2% in media-loaded (Fig. 7C) and 11 ± 6% ($p < 0.001$) in drop-loaded (Fig. 7D) samples. On day 3, the content of maturing elastic fibres in both methods of addition of tropoelastin was approximately 2% (drop-loaded 2.6 ± 0.8, media-loaded 2 ± 1.7%). This content of maturing elastic fibres decreased to 1.2 ± 0.7% in drop-loaded and 1.7 ± 1.4% in media-loaded samples on day 7. After the second addition of tropoelastin, drop-loaded and media-loaded samples treated with tropoelastin presented a significantly higher quantity of maturing elastic fibres (12.3 ± 4.5% and 5.9 ± 2.4% respectively) in comparison to untreated samples (0.8 ± 1%) by day 14 (Fig. 7B). Comparing addition methods, the drop-loaded samples presented a higher coverage of elastin ($p < 0.001$) and maturing elastic fibres ($p < 0.001$) than the media-loaded samples on day 14. Additionally, after assessing the maturing elastic fibre alignment both groups treated with tropoelastin presented a disordered fibre arrangement as the directionality curves were relatively flat (Fig. 7C, D), if compared with the curves from the 2D elastogenesis model (Fig. 2C). With these results we can state that drop-loading tropoelastin directly onto cell-seeded FCG scaffolds before adding cell growth medium resulted in a better coverage of elastin and maturing elastic fibres on the scaffold surface.

3.2.2. *Consistent cell proliferation in FCG scaffolds treated with tropoelastin*

Having shown that drop-loading tropoelastin resulted in a better superficial distribution of elastin and maturing elastic fibres, cell proliferation, gene expression and mechanical testing assays were carried out only on drop-loaded samples. When measured, the rate of cell proliferation proved to be constant between untreated samples and those treated with tropoelastin, across all time points (Fig. 8). Three days after the addition of tropoelastin, the average dsDNA concentration was 175 ± 10 ng/ml for the untreated samples and 213 ± 8 ng/ml for the tropoelastin-treated samples. Untreated samples had a mean dsDNA concentration of 225 ± 10 ng/ml and the tropoelastin-treated samples 192 ± 20 ng/ml by day 7. After 14 days, the concentration of dsDNA remained consistent in both untreated (198 ± 15 ng/ml) and tropoelastin-treated (186 ± 26 ng/ml) groups.

3.2.3. *Tropoelastin-treated FCG scaffolds showed elastin gene expression*

RT-qPCR analysis presented in Fig. 9 showed that there was significant ELN upregulation (1.7 ± 0.7) on day 3. The addition of tropoelastin resulted in upregulation of FBN1 (1.5 ± 0.6) on day 7. Overall, there was stable upregulation of ELN and EBP on days 7 and 14. Furthermore, LOX1 did not change at the time points studied. Therefore, similarly to

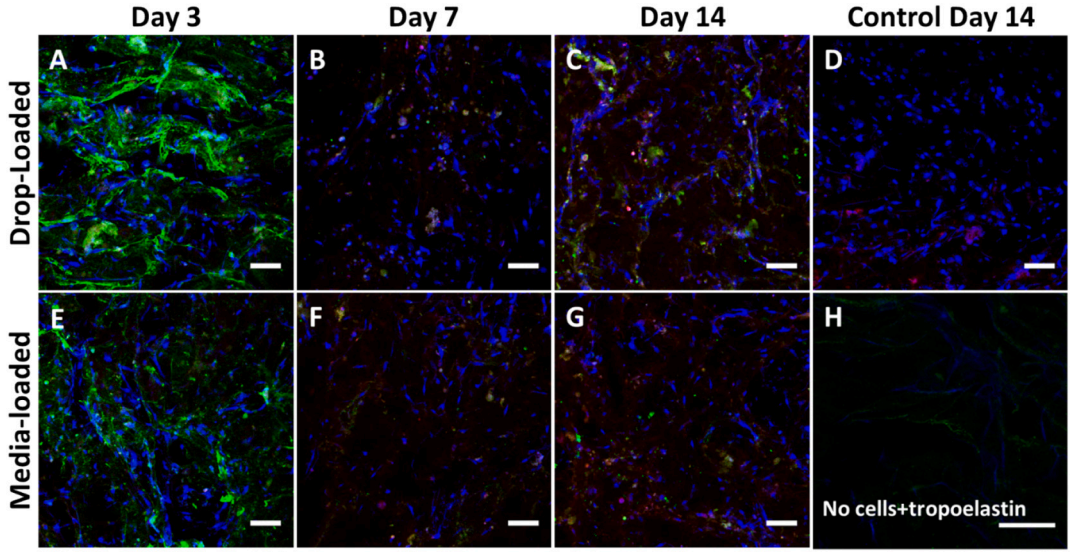

Fig. 6. Immunofluorescence of elastin (green) and autofluorescence at 561 nm of maturing elastic fibres (red) in FCG scaffolds according to the method of addition of tropoelastin. FCG scaffolds drop-loaded with tropoelastin on days (A) 3, (B) 7 and (C) 14. FCG scaffolds media-loaded with tropoelastin on day 3 (E), day 7 (F) and day 14 (G). There was an increase in maturing elastic fibre surface coverage on day 14 after second addition of tropoelastin. (D) FCG scaffolds with no tropoelastin added. (H) Acellular FCG scaffold treated with tropoelastin imaged on day 14. Blue = cell nuclei. Bar represents 100 μm in all images. (For interpretation of the references to colour in this figure legend, the reader is referred to the web version of this article.)

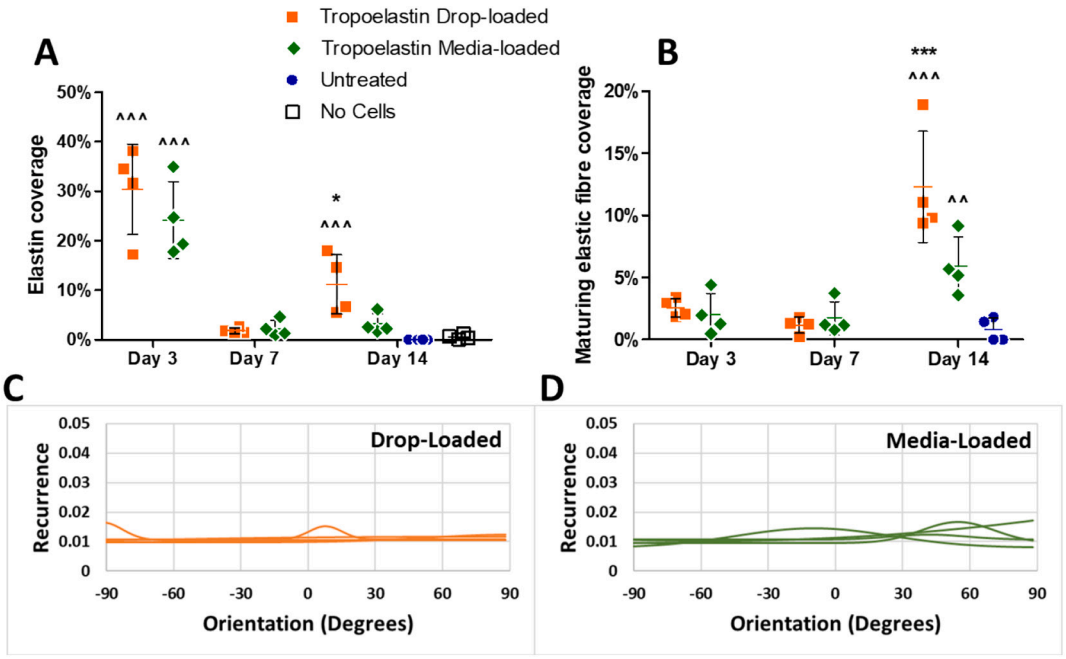

Fig. 7. Relative surface area coverage of elastin and maturing elastic fibres in FCG scaffolds. On day 14, drop-loaded and media-loaded samples presented a significantly higher quantity of maturing elastic fibres than untreated samples. Drop-loaded samples presented significantly higher content of (A) elastin and (B) maturing elastic fibres deposited if compared with media-loaded samples. Directionality curves of maturing elastic for (C) drop-loaded and (D) media-loaded samples on day 14. The curves are relatively flat, as there is no preferred elastic fibre orientation. (^^) $p < 0.01$, (^^^) $p < 0.001$ when compared to untreated samples. (*) $p < 0.05$, (***) $p < 0.001$ when compared to media-loaded samples at the same time point.

the 2D studies (Fig. 4), these 3D results indicate that elastogenesis was triggered after the addition of tropoelastin.

3.2.4. *No detrimental changes in mechanical properties and stable dimensional integrity of tropoelastin-treated FCG scaffolds*

Our next step was to analyse how the mechanical properties and dimensional integrity of the FCG scaffolds were influenced by the presence of elastin and maturing elastic fibres. Based on the data shown in Table 1, fourteen days after the addition of tropoelastin, the compressive and tensile modulus, ultimate tensile strength (UTS) and strain to failure of the samples treated with tropoelastin remained comparable to those of untreated samples.

Although no significant differences were observed in the stress-strain curves (Fig. 10A, B), in terms of compressive modulus (Fig. 10C), on day 14 the modulus of treated samples was lower (0.16 ± 0.02 kPa) than untreated samples (0.19 ± 0.1 kPa). At low strain (2–5% strain), by day

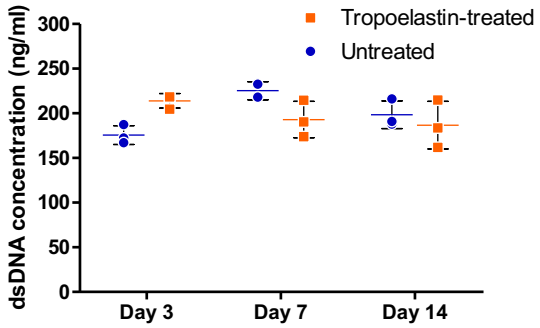

Fig. 8. dsDNA concentration in FCG scaffolds. No significant difference was observed in the rate of cell proliferation between untreated samples and samples treated with tropoelastin.

14 the average tensile modulus of tropoelastin-treated samples was 1.6 ± 0.3 kPa, when compared to untreated samples (1.8 ± 0.4 kPa). At high strain (10–15% strain), the modulus of the tropoelastin-treated samples was 5.8 ± 0.1 kPa (Fig. 10D). Additionally, scaffold tensile properties were examined with representative stress-strain curves. A small increase in treated samples UTS (64.7 ± 8.3 kPa) and strain to failure (17.1 ± 1.3%) was observed when compared against untreated samples. Furthermore, the standard deviations of the tropoelastin-treated samples were smaller than the untreated group. Finally, cell-mediated contraction was studied during two weeks and only a 2% decrease in diameter was observed in the tropoelastin-treated scaffolds, which is comparable to the untreated samples (Fig. 11A, B). These assessments have confirmed that the addition of tropoelastin did not affect negatively the mechanical properties of the FCG scaffolds and in addition to this, the scaffolds were capable of resisting cell-mediated contraction.

4. Discussion

Encouraging and controlling the production of new elastic fibres through elastogenesis is highly desirable in regenerative medicine, as elastic fibres prevent permanent tissue deformation while regulating phenotype, proliferation and migration in cells [3,30]. Therefore, the overall aim of this study was to activate elastogenesis in human vascular smooth muscle cells (hVSMCs) seeded in fibrin collagen glycosaminoglycan (FCG) scaffolds, by adding a solution of recombinant human tropoelastin. In this manuscript, we present a repeatable method to increase and tune elastogenesis by hVSMCs seeded in FCG scaffolds. hVSMCs were chosen as they are one of the principal elastogenic cells in the human body [49] however, hVSMCs are unable to produce elastin *in vitro* as they age when their passage increases [2]. Although hVSMCs and recombinant human tropoelastin have been previously used together in synthetic scaffolds [50], their combined elastogenic potential has never previously been examined. Additionally, unlike previous elastogenesis experiments involving SMCs [28,51], we have used a natural biomaterial scaffold and static cell culture. Here, elastogenesis was activated after the addition of tropoelastin and furthermore, the importance of a mature ECM to obtain enhanced deposition of elastin and maturing elastic fibres in tropoelastin-treated hVSMCs was shown. Moreover, we have demonstrated that the drop-loading of tropoelastin, resulted in maturing elastic fibre surface coverage, without affecting the cell

Table 1
Mechanical properties of FCG scaffolds treated with tropoelastin compared against untreated samples on day 14.

Mechanical properties at day 14	Tropoelastin	Untreated
Compressive modulus (kPa)	0.16 ± 0.02	0.19 ± 0.06
Low strain tensile modulus (2–5%, kPa)	1.6 ± 0.3	1.8 ± 0.4
High strain tensile modulus (10–15%, kPa)	5.6 ± 0.08	6.6 ± 2
Ultimate tensile strength (kPa)	64.7 ± 8.3	62 ± 19.3
Strain to failure (%)	17.1 ± 1.3	15.9 ± 0.8

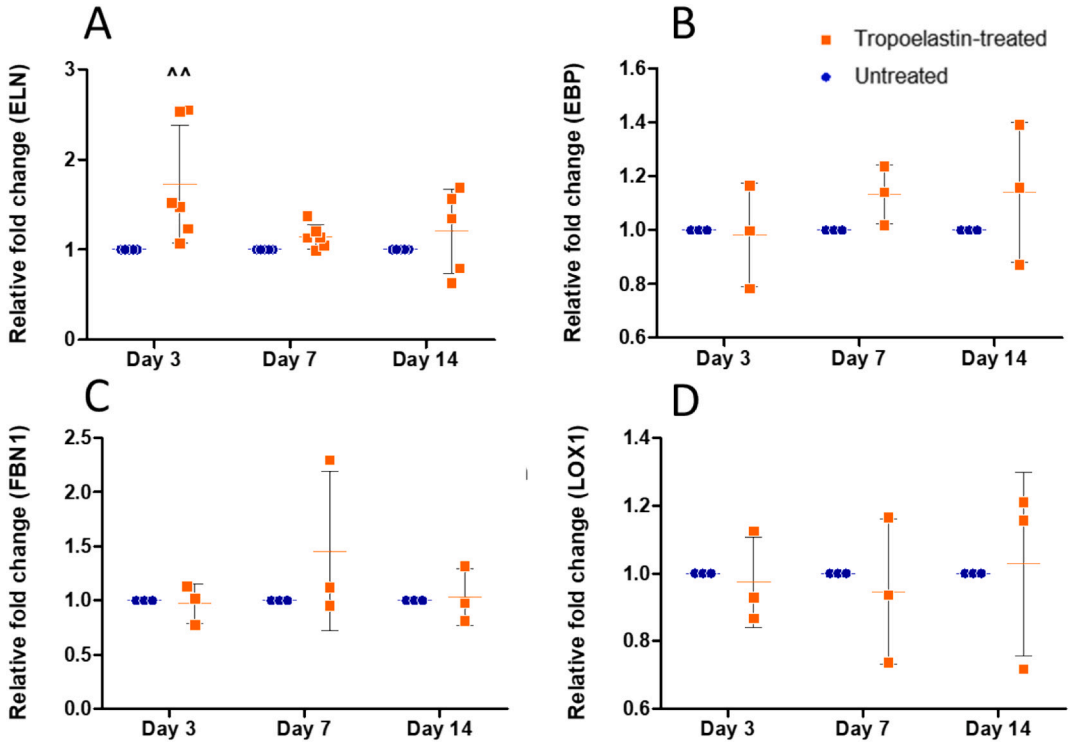

Fig. 9. Relative gene expression in FCG scaffolds. There was significant (A) ELN upregulation on day 3 of the experiment in samples treated with tropoelastin. No significant expression changes in (B) EBP, (C) FBN1 and (D) LOX1 genes were measured. (^^) $p < 0.01$, when compared to untreated sample.

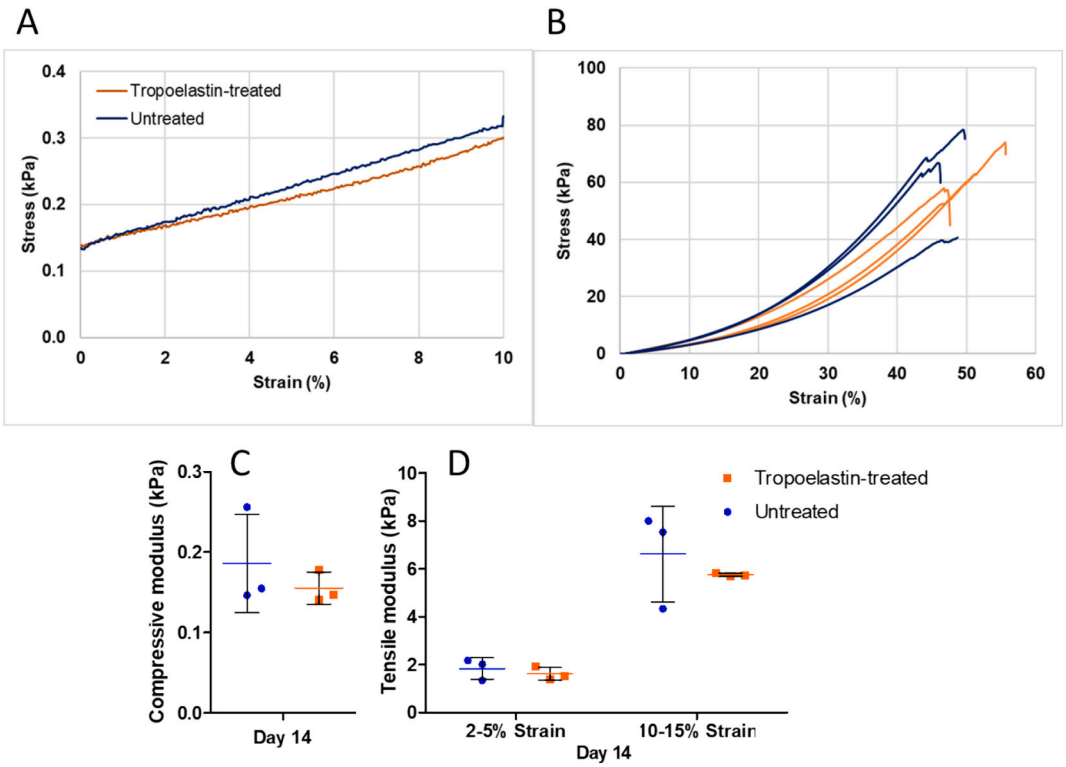

Fig. 10. Mechanical testing (compressive and tensile) of FCG scaffolds. There was a slight decrease in both moduli by the end of the experiment. (A) Average stress-strain curves for compressive testing on day 14. (B) Stress-strain curves obtained during tensile testing on day 14. (C) Compressive modulus of FCG scaffolds treated with tropoelastin, compared against untreated FCG scaffolds. By day 14, the average compressive moduli of treated samples was lower than the untreated samples. (D) Tensile modulus at low and high strain of FCG scaffolds on day 14. There was a decrease in modulus at low strain of 11.05% and 15.79% at high stain in tropoelastin-treated samples.

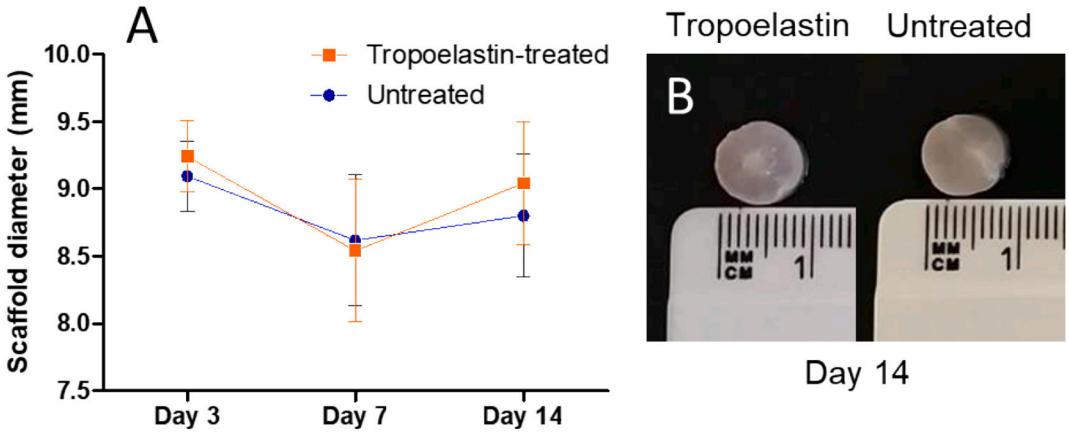

Fig. 11. Measurements of FCG scaffolds treated with tropoelastin showed no cell-mediated contraction. (A) There was no evidence of cell-mediated contraction in FCG scaffolds treated with tropoelastin, when compared to untreated samples. (B) Size of treated and untreated FCG scaffolds after 14 days.

proliferation in these scaffolds.

After assessing the best day for the addition of tropoelastin on hVSMCs seeded on glass slides, we could prove that ECM maturity affects the activation of elastogenesis. Waiting 10 days before adding tropoelastin to hVSMCs (A10 samples), led to a significant increase in the content of elastin and maturing elastic fibres than hVSMCs treated with tropoelastin directly after seeding (A0 samples). Furthermore, A10 samples presented globules of elastin showing bead-like patterns on day 3 (Fig. 1E); this type of pattern has been shown by Kozel et al. to be characteristic of the first stages of elastogenesis [52]. By day 7 (Fig. 1F), the coacervation of tropoelastin was obvious and the ECM was saturated in elastin. On day 14 the maturing elastic fibre alignment resembled lamellar-like structure very similar to the ones of the tunica media in arteries [5,53], and ventricularis layer in the leaflets of aortic heart valves [54]. To prove this point, a directionality analysis was carried out (Fig. 2C), showing that the maturing elastic fibres were aligned. Although this was undoubtedly a feature of the hVSMCs used here, it was nonetheless encouraging. From these results, it can be inferred that the limiting factor in elastin deposition may be the content of ECM-associated proteins (fibulins [55,56], fibrillins [57], and microfibrillar associate proteins [58]). We speculate that in the A0 samples, as tropoelastin was added after cell seeding, the microfibrillar mesh in the ECM was not fully formed, being unable to accommodate all the coacervated elastin, resulting in the loss of elastin during each growth

medium change. This has also been observed by Kozel et al., showing that elastin is unable to transform into an elastic fibre if there is no presence of ECM [59]. Additionally, looking at the RT-qPCR results (Fig. 4) all the elastin and maturing elastic fibres present in the ECM were as a result of introducing the tropoelastin. We can assume this as the levels of elastin (ELN) and LOX1 remained downregulated, whereas Fibrillin-1 (FBN1) and EBP were upregulated. It is known that FBN1 is of one of the elastic-fibre associated proteins in the microfibrillar mesh responsible for signalling the assembly of mature elastic fibres in tissues [57]. Therefore, the upregulation of FBN1 on day 7 shown in Fig. 4 makes sense, as there was a corresponding increase in the deposition of maturing elastic fibres.

Having successfully used tropoelastin to induce elastogenesis in hVSMCs on glass slides, we translated these results into a 3D model using FCG scaffolds. After quantifying the amount of elastin deposited in drop-loaded and media-loaded samples, we observed that the deposition of elastin within the cell-seeded scaffolds occurred during the first 3 days of this study and no significant changes were observed after the second addition of tropoelastin on day 7 (Fig. 5). Additionally, while there was a reduction in elastin content during the experiment, the rate of loss was not significant. Furthermore, there were no significant differences in elastin content between drop-loaded and media-loaded samples. On the other hand, after visually assessing the scaffolds, we obtained twice the surface area coverage of maturing elastic fibres by drop-loading tropoelastin onto the cell-seeded FCG scaffolds, outperforming samples where the tropoelastin was diluted in growth medium (media-loaded). It is presumed that by drop-loading tropoelastin, the distribution of elastin and elastic fibres on the scaffold surface was higher as the tropoelastin solution was more concentrated when first in contact (for 10 min) with the hVSMCs. Initially, the concentration of tropoelastin was 10 mg/ml and when growth medium was added this reduced to 250 μg/ml in the wells. However, by day 7 there was a reduction in elastin and no visible maturing elastic fibres (Fig. 6B, F). This indicated that there was not enough ECM secreted by the hVSMCs to allow deposition of elastin on the surface of the FCG scaffolds. Interestingly, despite this, a second addition of tropoelastin resulted in an increase in elastin and maturing elastic fibre surface area coverage (Fig. 6C, G). By the end of the experiment the surface of the FCG scaffolds presented maturing branching elastic fibres along the scaffold pores, resembling the elastic fibre architecture present in lungs [10]. Fibre alignment was corroborated with a directionality analysis (Fig. 7C, D) and we saw that the maturing elastic fibres in both drop-loaded and media-loaded samples had no preferred orientation. These results imply that the hVSMCs had by this point secreted enough ECM-associated proteins to support elastin deposition and crosslinking on the surface of the FCG scaffold. To the best of our knowledge this is the first study presenting the drop-loading of tropoelastin on natural biomaterial cell-seeded scaffolds to induce and control elastogenesis *in vitro*.

Having shown that controlled elastogenesis was possible by drop-loading tropoelastin, we carried out compressive and uniaxial tensile testing on tropoelastin-treated FCG scaffolds and there were no detrimental changes in mechanical properties. We could see that the compressive modulus was lower in the samples treated with tropoelastin (Fig. 10C) and in terms of tensile properties, when collagen and elastic fibres began to straighten at low strain this resulted in a reduction of tensile modulus (Fig. 10D). Similar results were observed at high strain, presumably due to the elastic fibres transferring energy to the collagen fibres to prevent overstretching [48]. Additionally, there was also an increase in ultimate tensile strength and strain to failure (Table 1). It is also noteworthy that after two weeks *in vitro*, FCG scaffolds were dimensionally stable (Fig. 11B). This is an important attribute, as many biomaterial constructs need to be capable of maintaining their shape post-implantation.

Although the addition of tropoelastin resulted in an efficient way to induce the formation of maturing elastic fibres in our FCG scaffolds, we suggest that future work should focus on finding ways to further increase the overall content of elastic fibres. Indeed, the use of supplements such as microfibrillar associated protein 4 (MFAP4) [60], transforming growth factor-β1 (TGF-β1) [61,62] and LOX1 [63] are also known to induce a deposition of elastic fibres in fibroblasts and hVSMCs. Interestingly, Mithieux et al [31] obtained an increase in elastic fibre deposition using medium containing higher than usual ECM-associated proteins. Recently, the use of macromolecular crowding techniques [64] and cell co-culture with monocytes [65], have been used as alternatives to enhance the deposition of ECM-associated proteins with promising results. These techniques, in combination with dynamic conditioning, using a bioreactor, might promote gene upregulation in cells, thus improving elastic fibre deposition, ECM and cell proliferation [66–68] in FCG scaffolds.

This FCG scaffold used here has applications in soft tissue reconstruction, as it combines fibrin's wound-healing and remodelling properties [37], the anti-calcification properties of GAGs [69], with collagen. In this study, we have shown how tuneable amounts of elastic fibres can be obtained by adding tropoelastin to stimulate elastogenesis [70]. As it stands, the current mechanical properties of this construct makes it suitable as a platform for skin [71] and lung alveolar wall regeneration [72], and tunica media repair in blood vessels [36].

5. Conclusions

We have successfully demonstrated that elastogenesis can be activated in the extracellular matrix (ECM) of cell-seeded scaffolds fabricated from fibrin, collagen and glycosaminoglycan (FCG) by adding recombinant human tropoelastin. We have proven the importance of cell density and having an ECM before adding tropoelastin for the deposition of maturing elastic fibres in human vascular smooth muscle cells (hVSMCs). It was observed that this technique allows the deposition of elastin and formation of lamellar maturing elastic fibres, like the ones found in skin, blood vessels and heart valves. Improved surface coverage of maturing branched elastic fibres can be achieved by drop-loading tropoelastin onto cell-seeded FCG scaffolds prior adding growth medium. Additionally, we could see the impact of elastic fibres in terms of mechanical properties in the scaffolds. With these results, we have established a natural biomaterial scaffold that can undergo controlled elastogenesis on demand, suitable for tissue engineering applications.

CRediT authorship contribution statement

Francisco R. Almeida-González: Conceptualisation, Methodology, Formal Analysis, Investigation, Data Curation, Writing – Original Draft, Visualisation, Funding Acquisition. **Arlyng González-Vázquez**: Methodology, Writing - Review & Editing, Supervision. **Suzanne M. Mithieux**: Resources, Writing - Review & Editing. **Fergal J. O'Brien**: Resources, Writing - Review & Editing, Supervision. **Anthony S. Weiss**: Conceptualization, Resources, Writing - Review & Editing. **Claire M. Brougham**: Conceptualisation, Methodology, Writing - Review & Editing, Visualisation, Supervision, Funding Acquisition.

Declaration of competing interest

The authors declare that they have no known competing financial interests or personal relationships that could have appeared to influence the work reported in this paper.

Acknowledgements

We would like to thank Dr. Brenton Cavanagh (RCSI) for confocal microscopy imaging and Dr. Pedro Jose Gouveia (RCSI) for help with the tensile testing. FRAG is the recipient of the TU Dublin Fiosraigh Dean of Graduate Research School Award and the TU Dublin School of Design and Mechanical Engineering provided financial support to this study.

References

[1] S.G. Wise, G.C. Yeo, M.A. Hiob, J. Rnjak-Kovacina, D.L. Kaplan, M.K.C. Ng, A. S. Weiss, Tropoelastin: a versatile, bioactive assembly module, Acta Biomater. 10 (2014) 1532–1541, https://doi.org/10.1016/j.actbio.2013.08.003.

[2] W.C. Parks, A.P. Richard, A.L. Katherine, R.P. Mecham, Elastin, 1993.

[3] S.K. Karnik, A critical role for elastin signaling in vascular morphogenesis and disease, Development. 130 (2003) 411–423, https://doi.org/10.1242/dev.00223.

[4] S.N. Angelov, J. Zhu, J.H. Hu, D.A. Dichek, What's the skinny on elastin deficiency and supravalvular aortic stenosis? Arterioscler. Thromb. Vasc. Biol. 37 (2017) 740–742, https://doi.org/10.1161/ATVBAHA.117.309257.

[5] M.J. Sherratt, Tissue elasticity and the ageing elastic fibre, Age (Omaha). 31 (2009) 305–325, https://doi.org/10.1007/s11357-009-9103-6.

[6] B. Vrhovski, A.S. Weiss, Biochemistry of tropoelastin, Eur. J. Biochem. 258 (1998) 1–18, https://doi.org/10.1046/j.1432-1327.1998.2580001.x.

[7] C.K. Breuer, B.A. Mettler, T. Anthony, V.L. Sales, F.J. Schoen, J.E. Mayer, Application of tissue-engineering principles toward the development of a semilunar heart valve substitute, Tissue Eng. 10 (2004) 1725–1736, https://doi.org/10.1089/ten.2004.10.1725.

[8] H. Tseng, K.J. Grande-Allen, Elastic fibers in the aortic valve spongiosa: a fresh perspective on its structure and role in overall tissue function, Acta Biomater. 7 (2011) 2101–2108, https://doi.org/10.1016/j.actbio.2011.01.022.

[9] J. Uitto, Biochemistry of the elastic fibers in normal connective tissues and its alterations in diseases, J. Invest. Dermatol. 72 (1979) 1–10, https://doi.org/10.1111/1523-1747.ep12530093.

[10] C.M. Kielty, M.J. Sherratt, C.A. Shuttleworth, Elastic fibres, J. Cell Sci. 115 (2002) 2817–2828, https://doi.org/10.1111/j.1468-2494.2010.00574.x.

[11] J.H. Eoh, N. Shen, J.A. Burke, S. Hinderer, Z. Xia, K. Schenke-Layland, S. Gerecht, Enhanced elastin synthesis and maturation in human vascular smooth muscle tissue derived from induced-pluripotent stem cells, Acta Biomater. 52 (2017) 49–59, https://doi.org/10.1016/j.actbio.2017.01.083.

[12] R. Wang, J. Ozsvar, G.C. Yeo, A.S. Weiss, Hierarchical assembly of elastin materials, Curr. Opin. Chem. Eng. 24 (2019) 54–60, https://doi.org/10.1016/j.coche.2019.01.004.

[13] A. Hinek, M. Rabinovitch, 67-kD elastin-binding protein is a protective "companion" of extracellular insoluble elastin and intracellular tropoelastin, J. Cell Biol. 126 (1994) 563–574, https://doi.org/10.1083/jcb.126.2.563.

[14] W.F. Daamen, J.H. Veerkamp, J.C.M. van Hest, T.H. van Kuppevelt, Elastin as a biomaterial for tissue engineering, Biomaterials. 28 (2007) 4378–4398, https://doi.org/10.1016/j.biomaterials.2007.06.025.

[15] L. Debelle, A.M. Tamburro, Elastin: molecular description and function, Int. J. Biochem. Cell Biol. 31 (1999) 261–272, https://doi.org/10.1016/S1357-2725(98)00098-3.

[16] A. Hatano, H. Chiba, H.A. Moesa, T. Taniguchi, S. Nagaie, K. Yamanegi, T. Takai-Igarashi, H. Tanaka, W. Fujibuchi, CELLPEDIA: a repository for human cell information for cell studies and differentiation analyses, Database. 2011 (2011) 1–10, https://doi.org/10.1093/database/bar046.

[17] S. Mithieux, A.S. Weiss, Elastin, Adv. Protein Chem. 70 (2006) 437–461, https://doi.org/10.1016/S0065-3233(04)70013-3.

[18] G.C. Yeo, S.M. Mithieux, A.S. Weiss, The elastin matrix in tissue engineering and regeneration, Curr. Opin. Biomed. Eng. 6 (2018) 27–32, https://doi.org/10.1016/j.cobme.2018.02.007.

[19] C. Saitow, D.L. Kaplan, J.J. Castellot, Heparin stimulates elastogenesis: application to silk-based vascular grafts, Matrix Biol. 30 (2011) 346–355, https://doi.org/10.1016/j.matbio.2011.04.005.

[20] J.L. Long, R.T. Tranquillo, Elastic fiber production in cardiovascular tissue-equivalents, Matrix Biol. 22 (2003) 339–350, https://doi.org/10.1016/S0945-053X(03)00052-0.

[21] N. Sommer, M. Sattler, J.M. Weise, H. Wenck, S. Gallinat, F. Fischer, A tissue-engineered human dermal construct utilizing fibroblasts and transforming growth factor β1 to promote elastogenesis, Biotechnol. J. 8 (2013) 317–326, https://doi.org/10.1002/biot.201200209.

[22] S. Tajima, A. Hayashi, T. Suzuki, Elastin expression is up-regulated by retinoic acid but not by retinol in chick embryonic skin fibroblasts, J. Dermatol. Sci. 15 (1997) 166–172, https://doi.org/10.1016/S0923-1811(97)00598-7.

[23] C. Tukaj, J. Kubasik-Juraniec, M. Kraszpulski, Morphological changes of aortal smooth muscle cells exposed to calcitriol in culture, Med. Sci. Monit. 6 (2000) 668–674.

[24] M.J. Merrilees, B.A. Falk, N. Zuo, M.E. Dickinson, B.C.H. May, T.N. Wight, Use of versican variant V3 and versican antisense expression to engineer cultured human skin containing increased content of insoluble elastin, J. Tissue Eng. Regen. Med. 11 (2017) 295–305, https://doi.org/10.1002/term.1913.

[25] H. Almeida, R. Domingues, S.M. Mithieux, R.A. Pires, A.I. Gonçalves, M. Gomez-Florit, R.L. Reis, A.S. Weiss, M.E. Gomes, Tropoelastin coated tendon biomimetic scaffolds promote stem cell tenogenic commitment and deposition of elastin-rich matrix, ACS Appl. Mater. Interfaces. (2019) acsami.9b04616. doi:https://doi.org/10.1021/acsami.9b04616.

[26] H. Xie, L. Lucchesi, B. Zheng, E. Ladich, T. Pineda, R. Merten, C. Gregory, M. Rutten, K. Gregory, Treatment of burn and surgical wounds with recombinant human tropoelastin produces new elastin fibers in scars, J. Burn Care Res. 1 (2017), https://doi.org/10.1097/BCR.0000000000000507.

[27] G.C. Yeo, A.S. Weiss, Soluble matrix protein is a potent modulator of mesenchymal stem cell performance., Proc. Natl. Acad. Sci. U. S. A. (2019) 201812951. doi:https://doi.org/10.1073/pnas.1812951116.

[28] T. Sugiura, R. Agarwal, S. Tara, T. Yi, Y.U. Lee, C.K. Breuer, A.S. Weiss, T. Shinoka, Tropoelastin inhibits intimal hyperplasia of mouse bioresorbable arterial vascular grafts, Acta Biomater. 52 (2017) 74–80, https://doi.org/10.1016/j.actbio.2016.12.044.

[29] P. Lee, G.C. Yeo, A.S. Weiss, A cell adhesive peptide from tropoelastin promotes sequential cell attachment and spreading via distinct receptors, FEBS J. 284 (2017) 2216–2230, https://doi.org/10.1111/febs.14114.

[30] S.M. Mithieux, S.G. Wise, A.S. Weiss, Tropoelastin - a multifaceted naturally smart material, Adv. Drug Deliv. Rev. 65 (2013) 421–428, https://doi.org/10.1016/j.addr.2012.06.009.

[31] S.M. Mithieux, A.S. Weiss, Design of an elastin-layered dermal regeneration template, Acta Biomater. 52 (2017) 33–40, https://doi.org/10.1016/j.actbio.2016.11.054.

[32] T.J. Levingstone, A. Matsiko, G.R. Dickson, F.J. O'Brien, J.P. Gleeson, A biomimetic multi-layered collagen-based scaffold for osteochondral repair, Acta Biomater. 10 (2014) 1996–2004, https://doi.org/10.1016/j.actbio.2014.01.005.

[33] T.J. Levingstone, A. Ramesh, R.T. Brady, P.A.J. Brama, C. Kearney, J.P. Gleeson, F. J. O'Brien, Cell-free multi-layered collagen-based scaffolds demonstrate layer specific regeneration of functional osteochondral tissue in caprine joints, Biomaterials. 87 (2016) 69–81, https://doi.org/10.1016/j.biomaterials.2016.02.006.

[34] J.P. Gleeson, N.A. Plunkett, F.J. O'Brien, Addition of hydroxyapatite improves stiffness, interconnectivity and osteogenic potential of a highly porous collagen-based scaffold for bone tissue regeneration, Eur. Cells Mater. 20 (2010) 218–230. doi:10.22203/eCM.v020a18.

[35] W.A. Lackington, R.M. Raftery, F.J. O'Brien, In vitro efficacy of a gene-activated nerve guidance conduit incorporating non-viral PEI-pDNA nanoparticles carrying genes encoding for NGF, GDNF and c-Jun, Acta Biomater. 75 (2018) 115–128, https://doi.org/10.1016/j.actbio.2018.06.014.

[36] A.J. Ryan, F.J. O'Brien, Insoluble elastin reduces collagen scaffold stiffness, improves viscoelastic properties, and induces a contractile phenotype in smooth muscle cells, Biomaterials. 73 (2015) 296–307, https://doi.org/10.1016/j.biomaterials.2015.09.003.

[37] C.M. Brougham, T.J. Levingstone, S. Jockenhoevel, T.C. Flanagan, F.J. O'Brien, Incorporation of fibrin into a collagen-glycosaminoglycan matrix results in a scaffold with improved mechanical properties and enhanced capacity to resist cell-mediated contraction, Acta Biomater. 26 (2015) 205–214, https://doi.org/10.1016/j.actbio.2015.08.022.

[38] S.L. Martin, B. Vrhovski, A.S. Weiss, Total synthesis and expression in Escherichia coli of a gene encoding human tropoelastin, Gene. 154 (1995) 159–166, https://doi.org/10.1016/0378-1119(94)00848-M.

[39] S.A. Jensen, B. Vrhovski, A.S. Weiss, Domain 26 of tropoelastin plays a dominant role in association by coacervation, J. Biol. Chem. 275 (2000) 28449–28454, https://doi.org/10.1074/jbc.M004265200.

[40] J. Schindelin, I. Arganda-Carreras, E. Frise, V. Kaynig, M. Longair, T. Pietzsch, S. Preibisch, C. Rueden, S. Saalfeld, B. Schmid, J.-Y. Tinevez, D.J. White, V. Hartenstein, K. Eliceiri, P. Tomancak, A. Cardona, Fiji: an open-source platform for biological-image analysis, Nat. Methods 9 (2012) 676–682, https://doi.org/10.1038/nmeth.2019.

[41] V.L. Singer, L.J. Jones, S.T. Yue, R.P. Haugland, Characterization of PicoGreen reagent and development of a fluorescence-based solution assay for double-stranded DNA quantitation, Anal. Biochem. 249 (1997) 228–238, https://doi.org/10.1006/abio.1997.2177.

[42] K.J. Livak, T.D. Schmittgen, Analysis of relative gene expression data using real-time quantitative PCR and the $2-\Delta\Delta CT$ method, Methods. 25 (2001) 402–408, https://doi.org/10.1006/meth.2001.1262.

[43] F.J. O'Brien, B.A. Harley, I.V. Yannas, L. Gibson, Influence of freezing rate on pore structure in freeze-dried collagen-GAG scaffolds, Biomaterials. 25 (2004) 1077–1086, https://doi.org/10.1016/S0142-9612(03)00630-6.

[44] M.G. Haugh, M.J. Jaasma, F.J. O'Brien, The effect of dehydrothermal treatment on the mechanical and structural properties of collagen-GAG scaffolds, J. Biomed. Mater. Res. - Part A. 89 (2009) 363–369, https://doi.org/10.1002/jbm.a.31955.

[45] M.G. Haugh, C.M. Murphy, R.C. McKiernan, C. Altenbuchner, F.J. O'Brien, Crosslinking and mechanical properties significantly influence cell attachment, proliferation, and migration within collagen glycosaminoglycan scaffolds, Tissue Eng. Part A. 17 (2011) 1201–1208, https://doi.org/10.1089/ten.tea.2010.0590.

[46] K.A. Ahmann, J.S. Weinbaum, S.L. Johnson, R.T. Tranquillo, Fibrin degradation enhances vascular smooth muscle cell proliferation and matrix deposition in fibrin-based tissue constructs fabricated *in vitro*, Tissue Eng. Part A. 16 (2010) 3261–3270, https://doi.org/10.1089/ten.tea.2009.0708.

[47] B.A. Harley, J.H. Leung, E.C.C.M. Silva, L.J. Gibson, Mechanical characterization of collagen-glycosaminoglycan scaffolds, Acta Biomater. 3 (2007) 463–474, https://doi.org/10.1016/j.actbio.2006.12.009.

[48] A. Hasan, K. Ragaert, W. Swieszkowski, Š. Selimović, A. Paul, G. Camci-Unal, M.R. K. Mofrad, A. Khademhosseini, Biomechanical properties of native and tissue engineered heart valve constructs, J. Biomech. 47 (2014) 1949–1963, https://doi.org/10.1016/j.jbiomech.2013.09.023.

[49] S.G. Wise, A.S. Weiss, Tropoelastin, Int. J. Biochem. Cell Biol. 41 (2009) 494–497, https://doi.org/10.1016/j.biocel.2008.03.017.

[50] L. Nivison-Smith, A.S. Weiss, Alignment of human vascular smooth muscle cells on parallel electrospun synthetic elastin fibers, J. Biomed. Mater. Res. - Part A. 100 (A) (2012) 155–161, https://doi.org/10.1002/jbm.a.33255.

[51] K.-W. Lee, D.B. Stolz, Y. Wang, Substantial expression of mature elastin in arterial constructs, Proc. Natl. Acad. Sci. 108 (2011) 2705–2710, https://doi.org/10.1073/pnas.1017834108.

[52] B.A. Kozel, B.J. Rongish, A. Czirok, J. Zach, C.D. Little, E.C. Davis, R.H. Knutsen, J. E. Wagenseil, M.A. Levy, R.P. Mecham, Elastic fiber formation: a dynamic view of

extracellular matrix assembly using timer reporters, J. Cell. Physiol. 207 (2006) 87–96, https://doi.org/10.1002/jcp.20546.
[53] A. Patel, B. Fine, M. Sandig, K. Mequanint, Elastin biosynthesis: the missing link in tissue-engineered blood vessels, Cardiovasc. Res. 71 (2006) 40–49, https://doi.org/10.1016/j.cardiores.2006.02.021.
[54] S. Parvin Nejad, M.C. Blaser, J.P. Santerre, C.A. Caldarone, C.A. Simmons, Biomechanical conditioning of tissue engineered heart valves: too much of a good thing? Adv. Drug Deliv. Rev. 96 (2016) 161–175, https://doi.org/10.1016/j.addr.2015.11.003.
[55] N. Kobayashi, G. Kostka, J.H.O. Garbe, D.R. Keene, H.P. Bächinger, F.-G. Hanisch, D. Markova, T. Tsuda, R. Timpl, M.-L. Chu, T. Sasaki, A comparative analysis of the fibulin protein family, J. Biol. Chem. 282 (2007) 11805–11816, https://doi.org/10.1074/jbc.M611029200.
[56] T. Sasaki, W. Göhring, N. Miosge, W.R. Abrams, J. Rosenbloom, R. Timpl, Tropoelastin binding to fibulins, nidogen-2 and other extracellular matrix proteins, FEBS Lett. 460 (1999) 280–284, https://doi.org/10.1016/S0014-5793(99)01362-9.
[57] H. Zhang, Developmental expression of fibrillin genes suggests heterogeneity of extracellular microfibrils, J. Cell Biol. 129 (1995) 1165–1176, https://doi.org/10.1083/jcb.129.4.1165.
[58] B. Pilecki, A.T. Holm, A. Schlosser, J.B. Moeller, A.P. Wohl, A.V. Zuk, S. E. Heumüller, R. Wallis, S.K. Moestrup, G. Sengle, U. Holmskov, G.L. Sorensen, Characterization of microfibrillar-associated protein 4 (MFAP4) as a tropoelastin- and fibrillin-binding protein involved in elastic fiber formation, J. Biol. Chem. 291 (2016) 1103–1114, https://doi.org/10.1074/jbc.M115.681775.
[59] B.A. Kozel, C.H. Ciliberto, R.P. Mecham, Deposition of tropoelastin into the extracellular matrix requires a competent elastic fiber scaffold but not live cells, Matrix Biol. 23 (2004) 23–34, https://doi.org/10.1016/j.matbio.2004.02.004.
[60] S. Kasamatsu, A. Hachiya, T. Fujimura, P. Sriwiriyanont, K. Haketa, M.O. Visscher, W.J. Kitzmiller, A. Bello, T. Kitahara, G.P. Kobinger, Y. Takema, Essential role of microfibrillar-associated protein 4 in human cutaneous homeostasis and in its photoprotection, Sci. Rep. 1 (2011) 1–10, https://doi.org/10.1038/srep00164.
[61] Z.H. Syedain, R.T. Tranquillo, TGF-B1 diminishes collagen production during long-term cyclic stretching of engineered connective tissue: implication of decreased ERK signaling, J. Biomech. 44 (2011) 848–855, https://doi.org/10.1016/j.jbiomech.2010.12.007.
[62] B.K. Mann, R.H. Schmedlen, J.L. West, Tethered-TGF-β increases extracellular matrix production of vascular smooth muscle cells, Biomaterials. 22 (2001) 439–444, https://doi.org/10.1016/S0142-9612(00)00196-4.
[63] C.R. Kothapalli, A. Ramamurthi, Lysyl oxidase enhances elastin synthesis and matrix formation by vascular smooth muscle cells, J. Tissue Eng. Regen. Med. 3 (2009) 655–661, https://doi.org/10.1002/term.214.
[64] A. Satyam, P. Kumar, X. Fan, A. Gorelov, Y. Rochev, L. Joshi, H. Peinado, D. Lyden, B. Thomas, B. Rodriguez, M. Raghunath, A. Pandit, D. Zeugolis, Macromolecular crowding meets tissue engineering by self-assembly: a paradigm shift in regenerative medicine, Adv. Mater. 26 (2014) 3024–3034, https://doi.org/10.1002/adma.201304428.
[65] X. Zhang, C.A. Simmons, J. Paul Santerre, Paracrine signalling from monocytes enables desirable extracellular matrix accumulation and temporally appropriate phenotype of vascular smooth muscle cell-like cells derived from adipose stromal cells, Acta Biomater. 103 (2019) 129–141, https://doi.org/10.1016/j.actbio.2019.12.006.
[66] P. Amrollahi, L. Tayebi, Bioreactors for heart valve tissue engineering: a review, J. Chem. Technol. Biotechnol. 91 (2016) 847–856, https://doi.org/10.1002/jctb.4825.
[67] J. Zhao, M. Griffin, J. Cai, S. Li, P.E.M. Bulter, D.M. Kalaskar, Bioreactors for tissue engineering: an update, Biochem. Eng. J. 109 (2016) 268–281, https://doi.org/10.1016/j.bej.2016.01.018.
[68] S. Hinderer, N. Shen, L.-J. Ringuette, J. Hansmann, D.P. Reinhardt, S.Y. Brucker, E. C. Davis, K. Schenke-Layland, In vitro elastogenesis: instructing human vascular smooth muscle cells to generate an elastic fiber-containing extracellular matrix scaffold, Biomed. Mater. 10 (2015) 10, https://doi.org/10.1088/1748-6041/10/3/034102.
[69] A.R. Alfonso, S. Rath, P. Rafiee, M. Hernandez-Espino, M. Din, F. George, S. Ramaswamy, Glycosaminoglycan entrapment by fibrin in engineered heart valve tissues, Acta Biomater. 9 (2013) 8149–8157, https://doi.org/10.1016/j.actbio.2013.06.009.
[70] S.M. Mithieux, B. Aghaei-Ghareh-Bolagh, L. Yan, K.V. Kuppan, Y. Wang, F. Garces-Suarez, Z. Li, P.K. Maitz, E.A. Carter, C. Limantoro, W. Chrzanowski, D. Cookson, A. Riboldi-Tunnicliffe, C. Baldock, K. Ohgo, K.K. Kumashiro, G. Edwards, A. S. Weiss, Tropoelastin implants that accelerate wound repair, Adv. Healthc. Mater. 7 (2018) 1–12, https://doi.org/10.1002/adhm.201701206.
[71] H. Joodaki, M.B. Panzer, Skin mechanical properties and modeling: a review, Proc. Inst. Mech. Eng. Part H J. Eng. Med. 232 (2018) 323–343, https://doi.org/10.1177/0954411918759801.
[72] S.E. Dunphy, J.A.J. Bratt, K.M. Akram, N.R. Forsyth, A.J. El Haj, Hydrogels for lung tissue engineering: biomechanical properties of thin collagen-elastin constructs, J. Mech. Behav. Biomed. Mater. 38 (2014) 251–259, https://doi.org/10.1016/j.jmbbm.2014.04.005.